International Journal of Research
Available at http://internationaljournalofresearch.org/
p-ISSN: 2348-6848
e-ISSN: 2348-795X
Volume 02 Issue 03
April 2015

Study of in-Vitro Drug Release Profiles of Time-controlled Penta-layered Nanofiber Meshes

Syeda Um-i-Zahra[1]*

[1]*College of Chemistry, Chemical Engineering and Biotechnology, Donghua University, Shanghai 201620, P.R. China*

***Corresponding authors:** Syeda Um-i-Zahra, E-mail addresses: um.i.zahra@hotmail.com. Tel.: +86 21 15000428928; Fax: +86 21 33734421.*

Abstract

Electrospinning was initiated to fabricate time-controlled penta-layered nanofiber meshes which could show a multiphasic drug release. The drug ratio in each nanofiber mesh was kept persistent and each polymer content was electrospun at already determined time intervals. The drug release interval can be controlled by adjusting spinning time of each mesh. XRD and FTIR studies have been conducted to identify the state of drug and polymers, and also the chemical interactions between them respectively. In-vitro drug release profiles demonstrate that nanofiber meshes with distinct penta-layered morphological structure are capable of multiphasic drug release. Such type of time-controlled drug release system can provide a platform for the development of novel structures that can be used as multiphasic drug release systems.

Keywords: *Electrospinning, time-controlled, nanofiber meshes, cellulose acetate, diffusion behavior, multiphasic drug release.*

1. Introduction

Research in the field of nanotechnology is rapidly expanding and nanofibers are being explored for a variety of applications along with drug delivery and tissue engineering. Nano-product materials have been utilized in biomedical and chemical engineering fields since the report of fabrication of first drug loaded nanofiber by using electrospinning technique (Kenawy el et al., 2002). The process of electrospinning was derived from simple fluid (Weitao Zhou, 2011) to multiple fluids (Kidoaki, Kwon, & Matsuda, 2005) and is becoming more complex with the improvement in fiber spinning techniques. Usually fibers with diameters less than 1 μm are termed as nanofibers. They give connection between the nano and the macroscopic objects. Due to their extremely high surface to mass ratio possess several novel properties such as low density, high pore volume, variable pore size and distinctive mechanical properties. These outstanding properties of nanofibers have given a pathway to the progress of several non-woven applications (Kumbar, James, Nukavarapu, & Laurencin, 2008).

The major issue in the research of drug delivery is to innovate new methodology or new system for the combine delivery of multiple drugs having different pharmaceutical action mechanisms to achieve a time controlled

multiphasic drug delivery system. The combination of different drugs is widely used in clinical chemotherapy and proves to be beneficial because it reduces the extreme negative side-effects of drugs (Zhang, Wang, & Yang, 2011). An ideal drug delivery system (DDS) is considered to deliver multiple therapeutic agents after loading into polymeric or other matrices and that can be able to release different drugs at controlled time intervals.

Extensive research has been conducted to develop several nanomaterials and nano-biodevices. The purpose of their development is to deliver the therapeutic agents in safe and effective way to human body, to display specific drug targeting and reduce toxicity. For this reason many techniques have been used to prepare different sophisticated controlled DDS. One of these techniques includes electrospinning which proves to be beneficial for fabrication of nanofiber meshes of varying sizes from different kinds of polymers (Bhardwaj & Kundu, 2010). Also different polymers give varying drug release profiles in different experimental conditions. The electrospun products serve as drug delivery vehicles and tissue engineering scaffolds (Thakur, Florek, Kohn, & Michniak, 2008). They attracted a great deal of attention due to their unique properties such as biocompatibility, biodegradability, flexibility in their morphology and composition and high surface area to volume ratio. For several drug delivery applications, different electrospinning parameters need to be modified in order to meet the specific requirements. Wang et al. (Wang, Wang, Qiao, & Yin, 2010) shows the development of novel controlled drug release system for multiple drugs such as rhodamin B and naproxen, consisted of Chitosan nanoparticles/PCL composite electrospun nanofibers with core–sheath structures. Other techniques include the preparation of layer-by-layer capsules (Delcea, Mohwald, & Skirtach, 2011; Guo et al., 2014) and self-assembled shells (Ariga, Lvov, Kawakami, Ji, & Hill, 2011; Wohl & Engbersen, 2012), polyelectrolyte multilayers designed for delivery of anti-cancer drugs (Ramasamy et al., 2014) and for bone metastasis prevention (Daubine et al., 2009), multilayer hybrid micro-particles (Du, Shi, Shi, Zhang, & Cao, 2013), irradiated biodegradable films (Loo, Tan, Chow, & Lin, 2010) and bimodal drug release matrix tablets (Streubel, Siepmann, Peppas, & Bodmeier, 2000).

Drug concentration should be balanced under constant plasma levels, however it is difficult to achieve. For the systematic release of these drugs Cho et al. (Cho, Lee, & Hong, 2014) designed multilayer nanofilms that shows drug release profiles for anticancer drugs in programmable fashion. This multilayer thin film dramatically affects not only the release profiles but also the structure stability in protein rich serum condition. Recently, Huang et al. (Huang, Branford-White, Shen, Yu, & Zhu, 2012) designed tri-layered drug loaded nanofiber meshes which could achieve time-engineered biphasic release fabricated through sequential electrospinning. The drug release speed and duration was managed by designing special morphological characteristic of each component mesh and it was found that each mesh was exhibiting biphasic drug release profile. Thus sequential electrospinning proves to be a useful tool for the fabrication of hierarchical ordered structure of multilayered nanofiber meshes by using different polymers to acquire biphasic even multiphasic drug release (Kidoaki et al., 2005). To fabricate a multilayer system of drug release the polymers are electropsun one after

another sequentially to achieve a time-controlled release pattern. Following this technology different drugs can be loaded in each layer and controls their release at different time intervals by time-programmed dual release formulation (Okuda, Tominaga, & Kidoaki, 2010).

Cellulose acetate (CA) is one of the most important organic esters derived from cellulose is a linear polysaccharide which has many advantageous properties including biocompatibility, biodegradability, and regeneration (H. Deng, 2010). It is the acetate ester of cellulose, has been widely studied for a wide variety of potential applications in the form of electrospun nanofiber mats (Thitiwongsawet P, 2010; Zhou W, 2011). Such applications include as the separation and purification processes (Shibata, 2004), formation of edible nanofibrous thin films (S. Wongsasulak, 2010), as transdermal drug delivery systems (Wu, Branford-White, Zhu, Chatterton, & Yu, 2010), as affinity membranes (Z. Ma, 2005), as antimicrobial membranes (N.Y. Abou-Zeid, 2011) and as biosensor strips (Z. Khatri, 2012). It is selected because its nanofibrous mats have attracted a great deal of attention showing excellent properties such as it is thermally stable, chemically resistant and biodegradable. It has the flexibility of making composites by mixing with appropriate adhesives (Baek et al., 2011) and other polymers to produce polymer blends (Syeda Um-i-Zahra, 2014) for the development of novel drug delivery systems. Ethyl cellulose (EC) is also chosen as the model polymer. It is an inert, hydrophobic polymer and its properties such as lack of toxicity, stability during storage make it suitable for sustained release matrices (Huang LY, 2012); It is also used for microencapsulation purposes (Murtaza, 2012). Polyvinylpyrrolidone (PVP) is a hydrophilic filament-forming polymer with a wide variety of applications in medicine, food, pharmacy, and cosmetics (Yu, Branford-White, White, Li, & Zhu, 2010). The PVP fibers formed the basis of a fast dissolving drug delivery system capable of forming nanofiber meshes and improved dissolution profiles of poorly water-soluble drugs for possible oral delivery applications. Ketoprofen (KET) is selected as a model drug. It is a non-steroidal anti-inflammatory drug (NSAID), widely applied to alleviate pain and inflammation associated with tissue injury (W. Chengyao, 2011). There nano-composites or blends are prepared in order to reduce the delivery problems and gastrointestinal side effects by controlling the rate, duration and site of release (Babazadeh, 2008).

The objective of this study is to develop novel penta-layered nanofibrous meshes to achieve time-controlled multiphasic release using sequential electropsinning process. Individual fiber meshes were deposited on target collector to achieve a hierarchical ordered structure. It involves a single drug and three different rate-controlling polymers. Ketoprofen (KET) was chosen as a model drug and loaded in different layers. Cellulose acetate (CA) and ethyl cellulose (EC) are hydrophobic polymers while polyvinylpyrrolidone (PVP) is a hydrophilic polymer.

2. Experimental

2.1 Materials

Ketoprofen was purchased from Wuhan Fortuna Chemical Co., Ltd. (Hubei, China). Cellulose acetate (white powder; Mw = 100,000 Da) was purchased from Acros (NJ, USA) and used as received. Polyvinylpyrrolidone K30 (PVP K30, M = 58,000 Da) was obtained from Shanghai Yunhong Pharmaceutical Aids and Technology Co., Ltd. (Shanghai, China). Ethyl cellulose (EC, 6–9 mPa s) was obtained from Aladdin

Chemistry Co., Ltd. (Shanghai, China). Acetone, N,N-dimethylacetamide (DMAc), and anhydrous ethanol were purchased from Sinopharm Chemical Reagent Co., Ltd. (Shanghai, China). All other chemicals used were of analytical grade, and water was doubly distilled immediately before use.

2.2 Preparation of Electrospinning Solution

The concentration of CA, EC and PVP in the spinning solutions were fixed at 10% (w/v), 24% (w/v) and 35% (w/v), respectively. To investigate the effect of CA, EC and PVP content on the drug release of KET, the amount of drug is fixed at 1%. For making CA solution acetone, N, N-dimethylacetamide (DMAc), and anhydrous ethanol (6:2:2 v/v) were used. For making EC and PVP solutions only anhydrous ethanol (10ml v/v) was used. Mechanical stirring and persistent heating (50 ± 1, 8 h) were applied for at least 12 h to obtain homogeneous co-dissolved spraying solutions. The solutions were degassed with a SK5200H ultrasonator (350W, Shanghai Jinghong Instrument Co., Ltd. Shanghai, China) for 10 min before electrospinning.

2.3 Electrospinning Process

A high voltage power supply (Shanghai Sute Electrical CO., Ltd.) was used to provide high voltages in the range of 0–60 kV. To avoid air bubbles, electrospinning solutions were carefully loaded in a 5 mL syringe to which a stainless steel capillary metal-hub needle was attached. The inside diameter of the metal needle was 0.5 mm. The positive electrode of the high voltage power supply was connected to the needle tip and the grounded electrode was linked to a metal collector wrapped with aluminum foil. The electrospinning process was carried out under ambient conditions (21 ± 2 ◦C and relative humidity 57 ± 3%). A fixed electrical potential of 13 kV was applied across a fixed distance of 15 cm between the tip and the collector. The feed rate of solutions was controlled at 0.5–1.0 mL/h by means of a single syringe pump (KDS100 Cole-Parmer®, USA). The formed fiber meshes were dried for over 24 h at 40◦C under vacuum (320 Pa) in a DZF-6050 Electric Vacuum Drying Oven (Shanghai Laboratory Instrument Work Co. Ltd., Shanghai, China). This facilitated the removal of residual organic solvent and moisture.

2.4 Fabrication of penta-layered nanofiber meshes

Penta-layered drug-loaded nanofiber meshes were fabricated using sequential electrospinning as shown by the schematic diagram (see Fig. 1A). The process involves of different CA, EC and PVP solutions containing model drug of KET, which were constructed from the following component meshes (see Fig. 1B and C): (i) the first drug-loaded mesh (top side), (ii) the second drug-loaded mesh (second side), (iii) the third drug-loaded mesh (third side), (iv) the fourth drug loaded mesh (fourth side) and (v) the fifth drug loaded mesh (bottom side). The drug-loaded meshes were prepared using 10% (w/v) acetone, N,N-dimethylacetamide (DMAc), and anhydrous ethanol-CA, 24% (w/v) ethanol-EC and 35% (w/v) ethanol-PVP containing 1% of the drug.

International Journal of Research
Available at http://internationaljournalofresearch.org/
p-ISSN: 2348-6848
e-ISSN: 2348-795X
Volume 02 Issue 03
April 2015

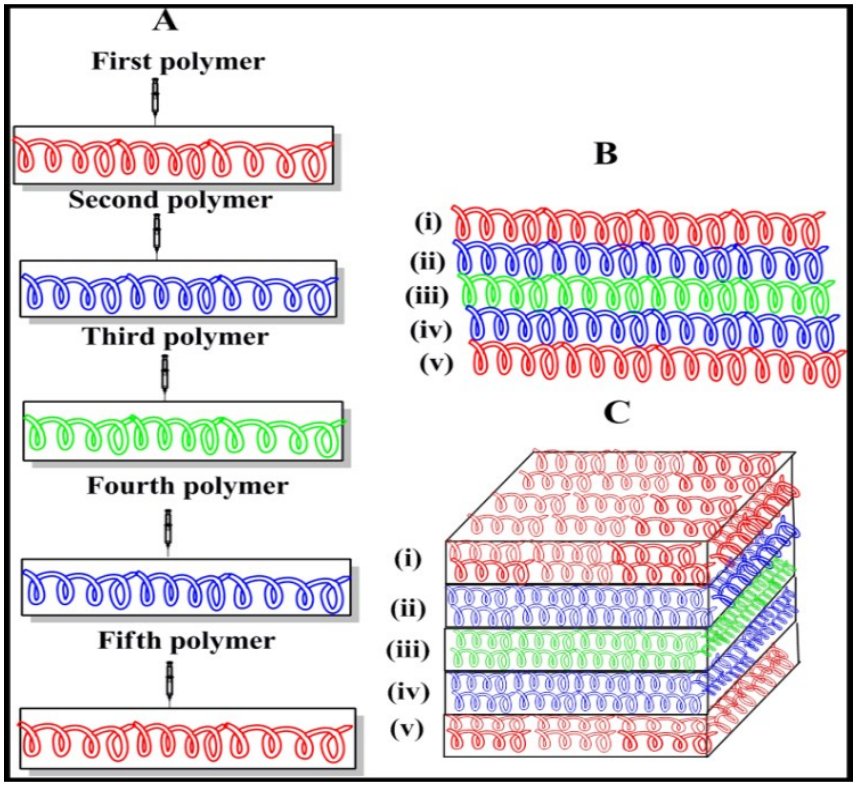

Fig. 1. Sequential electrospinning process (A) and graphical presentation of overview (B) and cross-sectional view (C)

These component meshes were prepared by electrospinning of KET-CA, KET-EC, KET-PVP successively under the applied conditions of 13 KV voltage, 0.5–1.0 mL/h flow rate, 15 cm air gap and spinning time were set different for different multilayers respectively. The preparation conditions for different composite nanofibers are shown in Table. 1.

Table 1: Preparation conditions for different composite nanofibers.

Group	Drug-polymer	Fiber mat	Polymer matrix	Drug (mg)	Polymer content (%)	Solvent
Group 1	KET-CA	F1	CA (Spinning time: 2h)	100	4	
	KET-CA	F2	CA (Spinning time: 2h)	100	6	Acetone
	KET-CA	F3	CA (Spinning time: 2h)	100	8	+
	KET-CA	F4	CA (Spinning time: 2h)	100	10	N,N-dimethyl
Group 2	KET-CA+KET-PVP+KET-EC+KET-PVP+KET-CA	F5	CA/PVP/EC/PVP/CA (Spinning time: 2h/2h/2h/2h/2h)	100	10/35/24/35/10	acetamide
(Penta-	KET-PVP+KET-EC+KET-CA+KET-EC+KET-PVP	F6	PVP/EC/CA/EC/PVP (Spinning time: 2h/2h/2h/2h/2h)	100	35/24/10/24/35	(DMAc)
layered	KET-CA+KET-EC+KET-PVP+KET-EC+KET-CA	F7	CA/EC/PVP/EC/CA (Spinning time: 2h/2h/2h/2h/2h)	100	10/24/35/24/10	+
meshes)	KET-PVP+KET-CA+KET-EC+KET-CA+KET-PVP	F8	PVP/CA/EC/CA/PVP (Spinning time: 2h/2h/2h/2h/2h)	100	35/10/24/10/35	Anhydrous
	KET-CA+KET-PVP+KET-EC+KET-PVP+KET-CA	F9	CA/PVP/EC/PVP/CA (Spinning time: 2h/4h/2h/4h/2h)	100	10/35/24/35/10	ethanol
	KET-PVP+KET-CA+KET-EC+KET-CA+KET-PVP	F10	PVP/CA/EC/CA/PVP (Spinning time: 2h/4h/2h/4h/2h)	100	35/10/24/10/35	

3. Characterization

3.1 Morphological analysis

The morphology of the nanofibers was assessed using an S-4800 field emission scanning electron microscope (FESEM) (Hitachi, Japan) and cross-sections of the multilayered meshes were assessed using an S-3400 field emission scanning electron microscope (FESEM) (Hitachi, Japan). Prior to the examination, the samples were platinum sputter-coated under a nitrogen atmosphere to render them electrically conductive. Images were recorded at an excitation voltage of 10 kV. The average fiber diameter was determined by measuring diameters of fibers at over 100 points from FESEM images using NIH Image J software (National Institutes of Health, MD, USA). The cross-sections of the nanofiber mats were prepared by first placing them into liquid nitrogen and then they were broken manually (C. B.-W. Deng-Guang Yu, Xia-Xia Shen, Xia-Fei Zhang, Li-Min Zhu, 2010; Yu et al., 2010).

3.2 X-ray diffraction studies

X-ray diffraction analysis (XRD) was obtained on a D/Max-BR diffractometer (RigaKu, Japan) with Cu Ka radiation in the 2 h range of 5–60° at 40 mV and 300 mA. The purpose of this method was used to investigate the state of the drug and polymers after they were electrospun into multilayered nanofibers.

3.3 FTIR

Fourier transform infrared (FTIR) analysis was carried out on a Nicolet-Nexus 670 FTIR spectrometer (Nicolet Instrument Corporation, Madison, USA) over the range, 500 cm^{-1} to 4000 cm^{-1} and a resolution of 2 cm^{-1}.

3.4 *In-Vitro* Release experiments

In-vitro dissolution tests were carried out according to the Chinese Pharmacopoeia (2005 ED.) Method II, a paddle method using a RCZ-8A dissolution apparatus (Tianjin University Radio Factory, China) was used. The dissolution medium consisted of 200 mL PBS buffer (pH 7.4). The temperature was maintained at 37°C ± 1 and the number of paddle rotations was adjusted to 50 rpm. Aliquots of 5 mL were taken at specific intervals and an equal amount of fresh dissolution medium was added to maintain a constant volume of the dissolution medium. The sample solutions were then analyzed at 260 nm by a UV spectrophotometer (Unico Instrument Co., Ltd., Shanghai, China). All the measurements were carried out in triplicate.

4. Results and discussions

4.1 Preparation of suitable spinning solutions

The concentration of CA in the spinning solutions was fixed at 10 (w/v) %. The trial process was as follows: we took acetic acid+3-times distilled water (8:2 v/v) as spinning solution at first. As a result electro-spraying takes place and round and globular microcapsules were observed instead of nanofibers. Then we tried acetone, N,N-dimethylacetamide (DMAc) and absolute ethanol (6:2:2 v/v). CA showed good compatibility with this binary solvent system, so an agreeable concentration of CA came as the next important reason. The amount of drug remains same in all spinning solutions i.e, 1%. SEM of different KET-CA concentrations was displayed in Fig. 2, (Left Panel). When the concentration of CA was 4%, a fluctuated flow sprayed and SEM showed numerous disordered beads with few fibers constructed (Fig. 2a). Increasing CA concentration to 6%, SEM exhibited non-uniform fibers with spindle-shaped beads (Fig. 2b). Continuing adding CA into the spinning solution to 8%, SEM portrayed more uniform fibers with less No. of round and spindle-shaped beads (Fig. 2c). Fairly well results came when CA concentration was 10%, SEM showed smooth and uniform fibers with nearly all beads absent (Fig. 2d).

According to SEM observations, the prepared fiber's diameters of KET-CA were measured, respectively, as F1=123.31±13nm, F2=116.79±17nm, F3=114.71±17nm and F4=107.38±17nm (Fig. 2, Right Panel). It was observed that as the

International Journal of Research
Available at http://internationaljournalofresearch.org/
p-ISSN: 2348-6848
e-ISSN: 2348-795X
Volume 02 Issue 03
April 2015

concentration of CA increased, the diameter of nanofibers gets decreased. The syringe needle, however, could be easily jammed with spinning solution if the flow rate was faster than 1.0 mL/h. It was therefore of great importance to maintain a proper flow rate and remove the residual spinning solution on the syringe needle at different time intervals. The concentration of PVP and EC in spinning solutions were kept as 35% and 24% respectively as studied before (Huang et al., 2012).

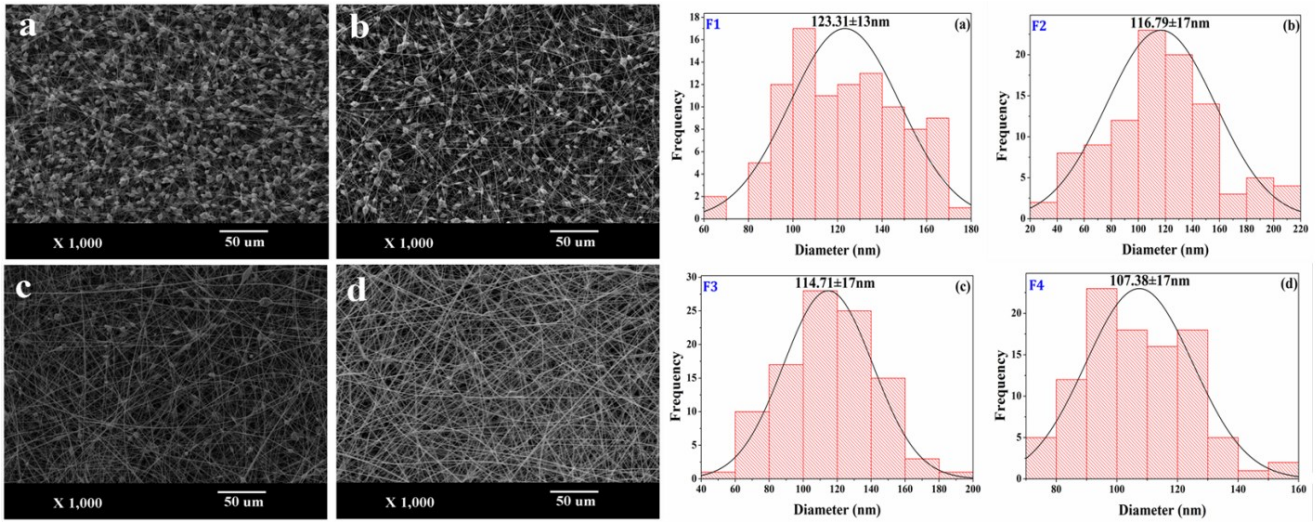

Fig. 2. SEM of preparation of KET-CA concentrations (a-d: CA concentration was 4% (F1), 6% (F2), 8% (F3), and 10% (F4), respectively, Left Panel). Graphs showing the diameter distribution of fiber mats (a-d: F1, F2, F3 and F4, Right panel)

4.2 Characterization and control of the release behaviors of penta-layer composite nanofiber meshes

To investigate the fiber diameters on the drug release profile, KET-CA mesh and penta-layer meshes with different polymer content were fabricated, respectively. Two groups of three different composite nanofibers were prepared (Table 1). It could be observed that meshes exhibit the most agreeable surface and uniformity.

The X-ray diffraction patterns for KET, CA, EC, PVP and four different penta-layered nanofiber meshes F5, F6, F7 and F8 are depicted in Fig. 3. The pure KET drug showed numerous sharp characteristic peaks appearing at diffraction angle of 2θ at 6.26°, 14.28°, 16.041°, 19.881°, 22.740° and 23.780° (C. B.-W. Deng-Guang Yu, Xia-Xia Shen, Xia-Fei Zhang, Li-Min Zhu, 2010), demonstrating the crystalline nature of the drug, whereas CA, EC and PVP showed diffused peaks indicating their amorphous characteristics. The XRD result for F5 penta-layered mesh revealed that the drug lost its diffraction peaks and polymers exhibited weakened characteristic peak intensity. This demonstrated that the drug had been uniformly dispersed in the polymer. Similar patterns were also obtained for F6, F7 and F8 nanofiber meshes suggesting that the drug is dispersed at the molecular level in the matrix and

hence, no crystals were found in them (Agnihotri, Mallikarjuna, & Aminabhavi, 2004).

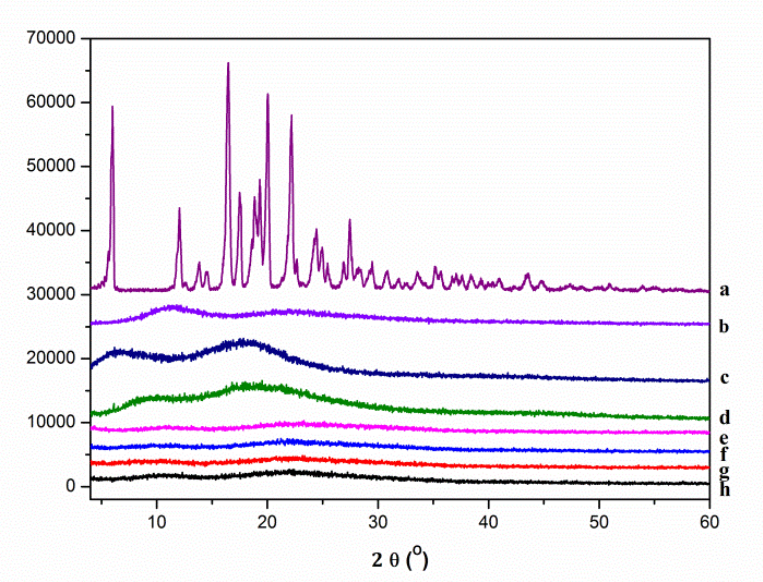

Fig. 3. XRD patterns of KET (a), PVP (b), EC (c), CA (d), F8 (e), F7 (f), F6 (g), and F5 (h).

The FTIR spectra for the pure KET drug, PVP, EC, CA and four different penta-layered nanofiber meshes F5, F6, F7 and F8 was done to establish drug-polymer compatibility and is given in Fig. 4. The FTIR spectrum for KET shows two distinct peaks of the C=O stretching around 1,697 cm^{-1} representing stretching vibrations of the carbonyl group in the KET dimer and 1655 cm^{-1} representing the stretching vibrations of the ketone group. The former was observed because KET molecules are bound together in dimers in its crystalline form. However, the peak at 1,697 cm^{-1} disappeared in the F8, F7, F6 and F5 nanofiber mesh, indicating the breakage of KET dimers and the formation of hydrogen bonds between the polymers and the hydroxyl group of KET (Fig. 4). So the compatibility among components is essential for producing high quality stable nanofibers.

The spectrum for EC demonstrated a distinct peak at 3464 cm^{-1}, which is due to the OH groups. The same also represents the intra- and intermolecular hydrogen bonding due to the OH groups (Li-Ya Huang, 2012). The asymmetric peak in the region 2970–2870 cm^{-1} may be due to CH stretching, and the peak at 1375 cm^{-1} is due to CH3 bending. The small peak near 1450 cm^{-1} is due to CH2 bending (Li-Ya Huang, 2012). Also KET has the C=O group and EC has the –OH groups presenting on the closed ring structure of the polymer's repeating units. So it is presumed that there will be interactions between the drug and polymer. KET molecules, by interacting with the polymer, are less likely to form dimers, which are essential for the formation of a crystal lattice.

The spectrum of PVP K30 shows, among others, important bands at 2955 cm^{-1} (C–H stretch) and 1662 cm^{-1} (C=O). A very broad band is also visible at 3438 cm^{-1} which is attributed to the presence of water (Yu et al., 2009).

Pure CA polymer showed two strong adsorption bands at 1752cm^{-1} and 1236cm^{-1}, which attributed to the C=O stretching and the acetyl groups,

respectively. According to He Jianxin (Jianxin He, 2007) the adsorption band at 1635cm-1 was assigned to the water adsorption, and 1371cm^{-1} and 1434 cm^{-1} were assigned to the symmetric and asymmetric vibrations of CH_3 (Weitao Zhou, 2011). CA molecules possess free hydroxyl groups (acting as potential proton donors for hydrogen bonding) and carbonyl groups (potential proton receptors) (X.-Y. L. Deng-Guang Yu, Xia Wang, Wei Chian, Yao-Zu Liao, Ying Li, 2013). Therefore, hydrogen bonding interactions can be speculated to occur within the KET-loaded CA, PVP and EC penta-layered nanofiber meshes. Although there may be secondary interactions between KET, CA, PVP and EC involving electrostatic and hydrophobic interactions through the KET benzene ring, it is thought to be mainly the hydrogen bonding interactions that prevent KET crystallization in the fibers. These interactions stabilize KET in an amorphous state in the nanofibers.

These FTIR results are in consistent with previous results having similar drug-polymer interactions (Yu, Yu, Chen, Williams, & Wang, 2012). Such interactions reflect the fine compatibility between drug and carrier polymer; they were useful for the stability of the drug in the ultrafine penta-layered nanofiber meshes and could also confer a dissolution rate advantage for ketoprofen.

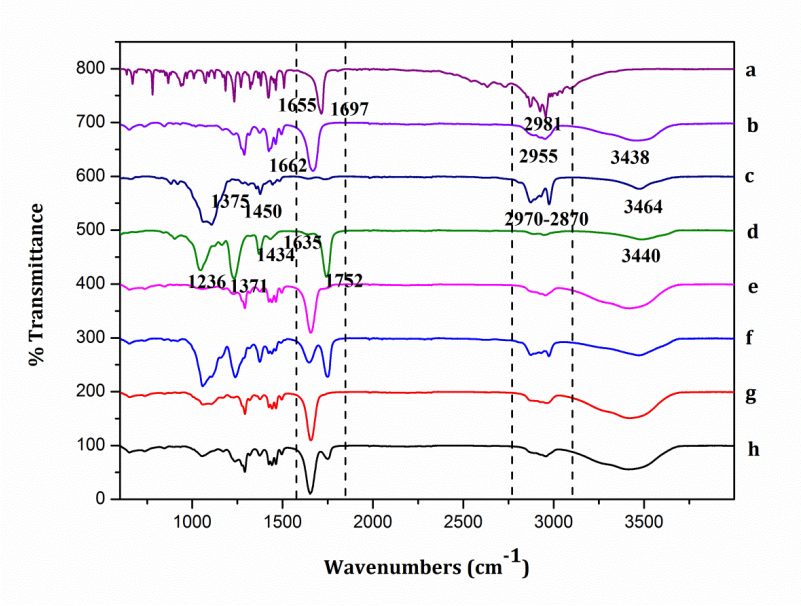

Fig. 4. FTIR spectra of KET (a), PVP (b), EC (c), CA (d), F8 (e), F7 (f), F6 (g) and F5 (h).

For the successful deposition of penta-layered nanofiber meshes it was essential to deposit layer by layer of each mesh through sequential electrospinning by exchanging different polymer solution at regular time intervals. To obtain a suitable morphological structure for penta-layered nanofiber mesh it requires much effort and it is very-time consuming task. Also it is very difficult to see all the five layers under very high magnification images of SEM. So for the visibility of five distinct layers SEM images were recorded at low magnification of X 100 (Fig. 5a). The end of a thread was smooth and neat indicating that the cross-section of penta-layered meshes was obtained from brittle rupturing manually other than cracking, which might greatly affected the morphology of the resultant meshes. Also the morphological appearances of these ends were round

and globular (Fig. 5b). When second layer is electrospun after the electrospinning of the first layer, electrostatic force of fibers would repel fibers received afterwards on the collector. As a result it became very difficult to place penta-layered nanofiber meshes into liquid nitrogen and then fragmented them physically to get their cross-section images.

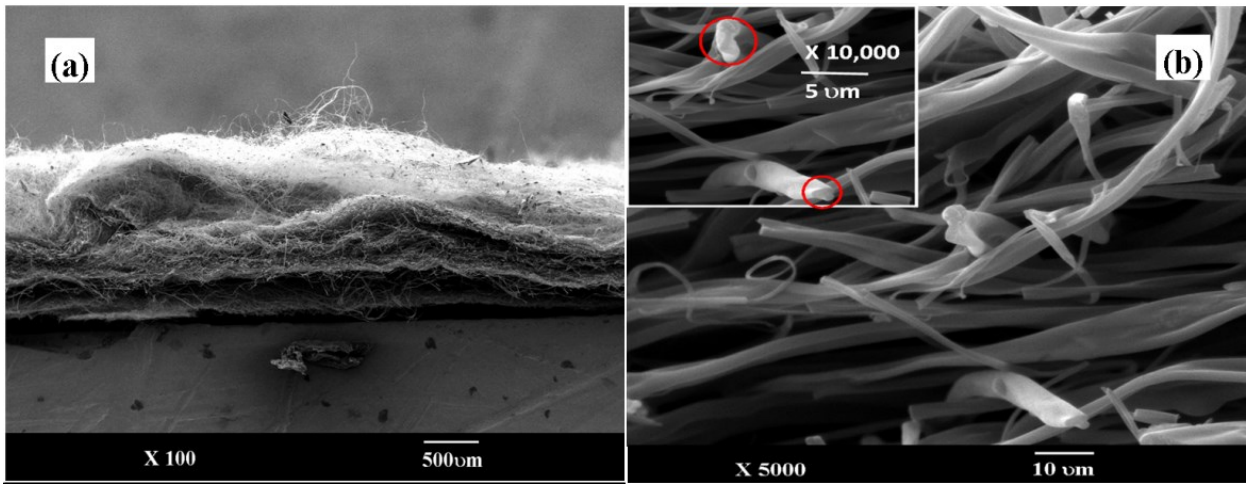

Fig. 5. SEM images of penta-layered nanofiber meshes at X 100 (a) and the end of threads of penta-layered meshes (b) (Red circle represents the end of a thread).

4.3 *In-vitro* drug release profiles

KET has a UV absorbance peak at 260 nm, hence, the amount of KET released from the fibers was determined by UV spectroscopy using a pre-determined calibration curve C = 15.27A–0.0034 (R = 0.9996) where C is the concentration of KET (g/mL^{-1}) and A is the solution absorbance at 260 nm (linear range: 2 to 20 g/mL^{-1}).

In-vitro drug release of KET-CA meshes F1, F2, F3 and F4 are shown in Fig 6. For F1, drug release showed sustained release profile and only about 25% of drug release was observed over 48 h periods. For F2 also sustained release was observed and about 40% drug release takes place within 48 h. For F3 and F4, 45% and 50% drug release was observed. So the maximum amount of drug release was shown by F4 nanofiber mats. This maximum amount of drug release was attributed to its more nanofibrous structure and beads nearly absent.

The ability of a drug to release from a polymer matrix depends on many factors, e.g., (i) the solubility of the drug in the polymer matrix and the testing medium, (ii) the swelling ability and the solubility of the polymer matrix in the testing medium, (iii) the diffusion of the drug from the polymer matrix, etc. Among these, the main contributing factors include the swelling and the solubility of the polymer matrix in the testing medium and the solubility of the drug in the polymer matrix. CA has been fabricated as semi-permeable membranes for separation processes and fibers and films for biomedical applications. It has also been used to prepare such nano-composites which showed water-repellent properties (Anitha, Brabu, John Thiruvadigal, Gopalakrishnan, & Natarajan, 2013).

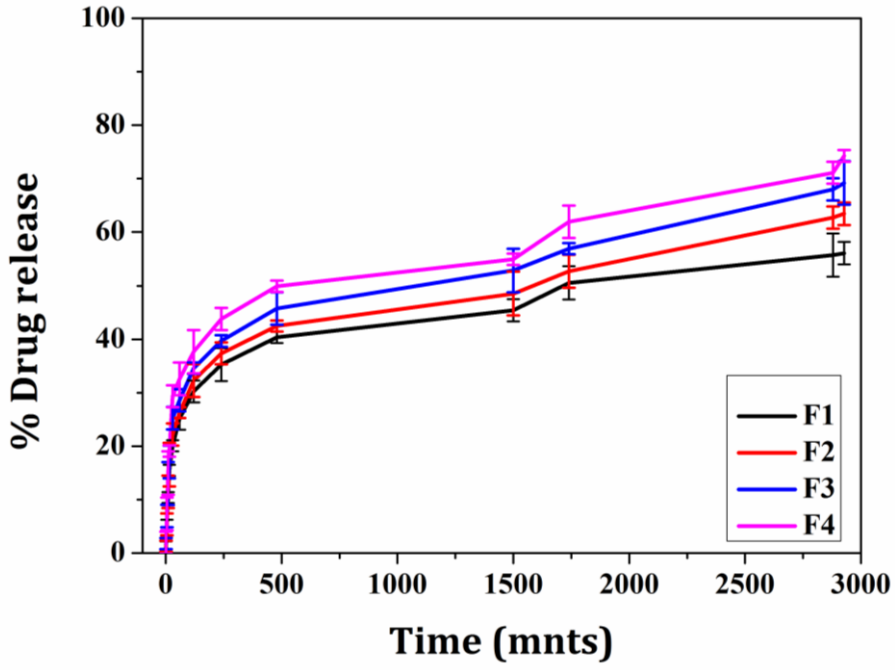

Fig. 6. Drug release from different KET-CA meshes (F1, F2, F3 and F4).

Fig. 7 showed the release behaviors of penta-layered meshes. The curve for F5 displayed a steady slope in the beginning for about 30 mints and then turned to a cliffy slope for the next 2h, then a mild stretch for about 5h they finally went up slightly and lasted for the following 16h, finally mild stretch for next few hours (Fig. 7a). This demonstrated that the drug experienced a little sustained release at first then moved into burst release period, then again sustained release for few hours. After that again burst release takes place for a long time and a final few hours of sustain release in the end. The curve for F6 showed a burst release of drug in the beginning and then a sustained release for about 15 h, finally again burst release was observed in the end (Fig. 7a). The curve for F7 displayed a sustained release profile of drug for about 2h, after that burst release occurred for 5h. Finally sustained release last for about 18-20h (Fig. 7a). The curve for F8 showed also a burst release profile in the first few minutes of drug release just like F6 and then a period of sustained release which lasts for about 15-16h, finally again burst release takes place in last few hours (Fig. 7a). F6 and F8 penta-layered meshes, however, exhibited slight differences in their sustained release period.

When increasing the spinning time of second and fourth phases of F5 and F8, which now labelled as F9 and F10 more specifically, drug released showed better release characteristics. The curve for F9 showed a mild steady slope in first few minutes and then immediately a burst release was observed (Fig 7b). The difference between F5 and F9 is that burst release takes place more in F9 because of longer spinning time. F9 release about 60% drug in burst release period. Then sustained release takes place for few hours. After this again burst release occurred and about 80% of drug release was observed. While in case of F5 62% drug released was observed. Finally sustained release takes place in last few hours. The curve for F10 (Fig 7b) showed a burst release profile in the beginning and about 62% drug was released. After few minutes it showed longer sustained release period because of presence of

hydrophobic polymers, finally after 16h it again showed burst release because of hydrophilic nature of PVP. About 85% of drug released occurred in this phase, while in case of F8 only 75% of drug release takes place in this phase. So this clearly demonstrated that more spinning time can result in more drug release from nanofiber meshes. If we increase the spinning time of PVP nanofiber meshes upto 6 hours or 8 hours we can expect even more burst release profiles of the drug.

This fact can be further described on the basis of more PVP content in second and fourth layers of F9, and first and last layers of F10, which are responsible for faster drug release from these meshes. This occurrence is deeply related with the hydrophilic nature of PVP which speed up the drug release rate. These results demonstrate that time-controlled multiphasic drug release can be achieved by designing penta-layered electrospun nanofiber meshes. Their drug release profiles can also be modified according to the requirement. Table 3 shows comparison of the release parameters of penta-layered nanofiber meshes.

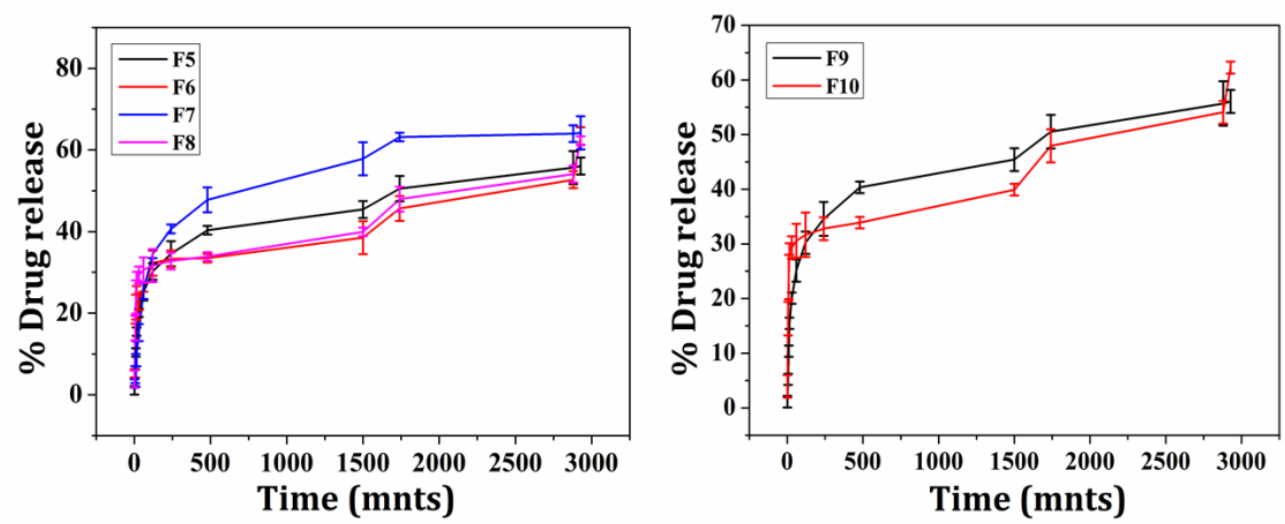

Fig. 7. Drug released from penta-layered meshes F5, F6, F7 and F8 with spinning time of 2h each mesh (a) and penta-layered meshes F9 and F8 with spinning time 2h/4h/2h/4h/2h (b).

To better understand the release mechanisms of the encapsulated KET from the penta-layered nanofiber meshes, the following Peppas equation has been successfully utilized. The Ritger–Peppas model was applied to describe drug release from matrix systems of various geometries by using a simple exponential relation (1), i.e.

$$M_t/M_\infty = Kt^n \quad \ldots\ldots\ldots\ldots\ldots\ldots (1)$$

where Mt is the drug released amount at time t, M∞ is the amount of drug released at infinite time, Mt/M∞ is the percentage of active ingredient released at time t, k is a kinetic constant that incorporates characteristics of the macromolecular network system and the active ingredient, and n is the diffusional exponent, indicative of the mechanism of drug release. The value of n is related to the geometrical shape of the formulation and determines the release mechanism.

International Journal of Research
Available at http://internationaljournalofresearch.org/
p-ISSN: 2348-6848
e-ISSN: 2348-795X
Volume 02 Issue 03
April 2015

According to this classification, there are four distinguishable modes of diffusion: (i) the value of n = 0.5 suggests Fickian or Case I transport behavior in which the relaxation coefficient is negligible during transient sorption; (ii) the value of n = 1 refers to a non-Fickian or Case II mode of transport where the morphological changes are abrupt; (iii) if 0.5 <n < 1, the transport process is anomalous, corresponding to Case III, and the structural relaxation is comparable to diffusion; (iv) a value of n < 0.5 indicates a pseudo-Fickian behavior of diffusion where sorption curves resemble Fickian curves, but the approach to final equilibrium is very slow. By plotting (M_t/M_∞) versus log (t), the n and k values as well as corresponding determination coefficients (R2) were obtained, as listed in Table 2.

Table 2: Release characteristics of encapsulated KET-CA (F1-F4) and penta-layered nanofiber mesh (F5-F10).

Nanofiber Mats	Drug loading amount (mg/ml)	Temperature (°C)	n	k	R^2
F1	100	25	0.168	0.843	0.955
F2	100	25	0.253	0.802	0.958
F3	100	37	0.279	0.883	0.883
F4	100	37	0.227	1.075	0.892
F5	100	25	0.002	1.657	0.805
F6	100	25	0.001	1.71	0.777
F7	100	25	0.002	1.665	0.688
F8	100	25	0.001	1.71	0.691
F9	100	37	0.004	1.686	0.898
F10	100	37	0.003	1.738	0.753

For the KET-CA nanofibrous mats F1-F4, the n values were found to be in the range of 0.168–0.279 at 37 ◦C, showing the pseudo-Fickian diffusion release mechanism. The release behavior resembles Fickian diffusion behavior, but it is very slow to reach final equilibrium, which may be attributed to the reason that the hydrophilic drug KET is difficult to diffuse out of hydrophobic KET-CA nanofibrous mats in PBS at 37 ◦C. In addition, the k value was found to increase with the decrease in CA amount, corresponding to the looser aggregate structure in the case of the lower CA amount. For penta-layered meshes i.e, from F5-510, the n values are found to be in the range of 0.001-0.008 at 37◦C also showing pseudo-Fickian diffusion release mechanism. The comparison of drug release (%) and release mechanisms for KET-CA and penta-layered nanofiber meshes are given in table 3. The Ritger–Peppas equations for penta-layered meshes are: F5: lnQ=0.002lnt+1.657 (r=0.4027), F6: lnQ=0.001lnt+1.71 (r=0.389), F7: lnQ=0.002lnt+1.665 (r=0.344), F8: lnQ=0.001lnt+1.71 (r=0.345), F9: lnQ=0.004lnt+1.686 (r=0.449), F10: lnQ=0.003lnt+1.738 (r=0.376). *In-vitro* release experiments demonstrated that drug release faster from PVP meshes while sustained release was observed from CA and EC polymer meshes in consecutive penta-layered meshes. Drug release speed and duration was controlled using morphological characteristics of each electrospun mesh, such as mesh thickness and spinning time.

Table 3: Comparison of the drug release (%) and release mechanism of encapsulated KET-CA (F1-F4) and penta-layered nanofiber meshes (F5-F10).

Fiber mat	Time, t	Drug release (%)	Release mechanism
F1	1min	10	Diffusion
F2	1min	10	Diffusion
F3	1min	10	Diffusion
F4	1min	13	Diffusion
F5	24h	49/50.1/56/58/64	Multiphasic release
F6	24h	49/57/57/60/68	Multiphasic release
F7	24h	49/50/66/66/67	Multiphasic release
F8	24h	49/58/59/60/69	Multiphasic release
F9	48h	49/58/58.5/64/64	Multiphasic release
F10	48h	56/58/59/60/69	Multiphasic release

Mostly biomolecules, drugs and other therapeutic agents have different times of degradation or different half-lives. An optimal controlled-release delivery system should be capable of being loaded with different levels of therapeutic agents for use in different medical symptoms. To develop such kind of time-controlled drug delivery system, electrospinning has been widely used to fabricate multilayered drug loaded nanofiber meshes which are capable of controlled release at regular time intervals. Several studies have been reported in which controlled release drug delivery systems have been prepared using electrospun nanofibrous meshes (Kim et al., 2004; Maretschek, Greiner, & Kissel, 2008; Murakami, Kobayashi, Takeuchi, & Kawashima, 2000; Singh et al., 2001; Yan, Xiaoqiang, Shuiping, Xiumei, & Ramakrishna, 2009). Advance research is focused on the development of highly efficient, multiphasic drug release systems. As described in this study, by controlling mesh thickness and spinning time, a penta-layered drug delivery system could be developed to achieve multiphasic drug release. These parameters could be regulated and designed according to the requirements. The time-controlled multiphasic drug release system described in this study is capable (i) for the development of more advanced and more efficient controlled-release drug delivery system and tissue engineering devices (ii) could provide multiphasic drug release profiles for single and multiple drugs (iii) sequential drug delivery of different drug combinations (iv) different proteins, hormones, growth factors and therapeutic agents can be embedded in this kind of hierarchical nano architecture (v) can be applied to deliver a continuous release of antagonistic compounds, which can inhibit infections and (vi) can develop different miscible/non-miscible polymer blends or nanoconjugates for combine drug delivery systems. Thus this approach proves to be promising for the local multiphasic delivery of anti-inflammatory an/anti-tumor drugs to targeted sites in the body.

5. Conclusion

This study demonstrates the best use of time-controlled multiphasic drug release systems using penta-layered nanofiber meshes. SEM images showed that single layer nanofibers of KET-CA with 10% CA concentration have better morphological features, however penta-layered meshes could be

fabricated by exchanging different polymers at preset time intervals. XRD results of penta-layered nanofiber meshes (F5-F10) revealed that drug is dispersed at the molecular level in these polymer matrixes and changes from crystalline to amorphous state. FTIR studies suggest that ketoprofen drug shows good compatibility and hydrogen bonding with cellulose acetate, ethyl cellulose and polyvinylpyrrolidone polymers respectively. *In-vitro* drug release profiles showed that KET-CA (F1-F4) nanofibers show sustained release mechanism which follows a pseudo-Fickian behavior of diffusion. For penta-layered (F5-F10) nanofiber meshes, *in-vitro* drug release profiles showed that burst release takes place from PVP matrixes while sustained release takes place from CA and EC matrixes. It is revealed that drug release speed, duration and time interval could be adjusted by controlling the morphological features of electrospun meshes such as thickness and spinning time. The time-controlled multiphasic drug release system described in this study is promising and can be used for the development of other novel, biomedical and pharmaceutical controlled-release drug delivery vehicles.

Acknowledgements: This work was supported by the Langsha Group, Jofo (WeiFang) Nonwoven Co. Ltd and the UK-CHINA Joint Laboratory for Therapeutic Texiles.

References

[1] Agnihotri, S. A., Mallikarjuna, N. N., & Aminabhavi, T. M. (2004). Recent advances on chitosan-based micro- and nanoparticles in drug delivery. *J Control Release, 100*(1), 5-28. doi: 10.1016/j.jconrel.2004.08.010

[2] Anitha, S., Brabu, B., John Thiruvadigal, D., Gopalakrishnan, C., & Natarajan, T. S. (2013). Optical, bactericidal and water repellent properties of electrospun nano-composite membranes of cellulose acetate and ZnO. *Carbohydr Polym, 97*(2), 856-863.

[3] Ariga, K., Lvov, Y. M., Kawakami, K., Ji, Q., & Hill, J. P. (2011). Layer-by-layer self-assembled shells for drug delivery. *Adv Drug Deliv Rev, 63*(9), 762-771. doi: 10.1016/j.addr.2011.03.016

[4] Babazadeh, M. (2008). Design, synthesis and in vitro evaluation of vinyl ether type polymeric prodrugs of ibuprofen, ketoprofen and naproxen. *Int J Pharm, 356*(1-2), 167-173. doi: 10.1016/j.ijpharm.2008.01.003

[5] Baek, W. I., Pant, H. R., Nam, K. T., Nirmala, R., Oh, H. J., Kim, I., & Kim, H. Y. (2011). Effect of adhesive on the morphology and mechanical properties of electrospun fibrous mat of cellulose acetate. *Carbohydr Res, 346*(13), 1956-1961. doi: 10.1016/j.carres.2011.05.025

[6] Bhardwaj, N., & Kundu, S. C. (2010). Electrospinning: a fascinating fiber fabrication technique. *Biotechnol Adv, 28*(3), 325-347. doi: 10.1016/j.biotechadv.2010.01.004

[7] Cho, Y., Lee, J. B., & Hong, J. (2014). Controlled release of an anti-cancer drug from DNA structured nano-films. *Sci Rep, 4*, 4078. doi: 10.1038/srep04078

[8] Daubine, F., Cortial, D., Ladam, G., Atmani, H., Haikel, Y., Voegel, J. C., . . . Benkirane-Jessel, N. (2009). Nanostructured polyelectrolyte multilayer drug delivery systems for bone metastasis prevention. *Biomaterials, 30*(31), 6367-6373. doi: 10.1016/j.biomaterials.2009.08.002

[9] Delcea, M., Mohwald, H., & Skirtach, A. G. (2011). Stimuli-responsive LbL capsules

and nanoshells for drug delivery. *Adv Drug Deliv Rev, 63*(9), 730-747. doi: 10.1016/j.addr.2011.03.010

[10] Deng-Guang Yu, C. B.-W., Xia-Xia Shen, Xia-Fei Zhang, Li-Min Zhu. (2010). Solid dispersions of ketoprofen in drug-loaded electrospun nanofibers. *Journal of Dispersion Science and Technology, 31*(7), 902-908.

[11] Deng-Guang Yu, X.-Y. L., Xia Wang, Wei Chian, Yao-Zu Liao, Ying Li. (2013). Zero-order drug release cellulose acetate nanofibers prepared using coaxial electrospinning. *Cellulose, 20*(379-389).

[12] Du, C., Shi, J., Shi, J., Zhang, L., & Cao, S. (2013). PUA/PSS multilayer coated CaCO3 microparticles as smart drug delivery vehicles. *Mater Sci Eng C Mater Biol Appl, 33*(7), 3745-3752. doi: 10.1016/j.msec.2013.05.004

[13] Guo, H., Guo, Q., Chu, T., Zhang, X., Wu, Z., & Yu, D. (2014). Glucose-sensitive polyelectrolyte nanocapsules based on layer-by-layer technique for protein drug delivery. *J Mater Sci Mater Med, 25*(1), 121-129. doi: 10.1007/s10856-013-5055-6

[14] H. Deng, X. Z., X. Wang, C. Zhang, B. Ding, Q. Zhang, Y. Du. (2010). Layer-by-layer structured polysaccharides film-coated cellulose nanofibrous mats for cell culture. *Carbohydrate Polymers, 80*(2), 474–479.

[15] Huang, L. Y., Branford-White, C., Shen, X. X., Yu, D. G., & Zhu, L. M. (2012). Time-engineeringed biphasic drug release by electrospun nanofiber meshes. *Int J Pharm, 436*(1-2), 88-96. doi: 10.1016/j.ijpharm.2012.06.058

[16] Huang LY, Y. D., Branford-White C, Zhu LM. (2012). Sustained release of ethyl cellulose micro-particulate drug delivery systems prepared using electrospraying. *Journal of material science, 47*, 1372-1377.

[17] Jianxin He, Y. T., Shan-Yuan Wang. (2007). Differences in morphological characteristics of bamboo fibers and other natural cellulose fibers: studies on X-ray diffraction, solid state 13C-Cp/MAS NMR, and second derivative FTIR spectroscopy data. *Iranian polymer journal, 16*(12), 807-818.

[18] Kenawy el, R., Bowlin, G. L., Mansfield, K., Layman, J., Simpson, D. G., Sanders, E. H., & Wnek, G. E. (2002). Release of tetracycline hydrochloride from electrospun poly(ethylene-co-vinylacetate), poly(lactic acid), and a blend. *J Control Release, 81*(1-2), 57-64.

[19] Kidoaki, S., Kwon, I. K., & Matsuda, T. (2005). Mesoscopic spatial designs of nano- and microfiber meshes for tissue-engineering matrix and scaffold based on newly devised multilayering and mixing electrospinning techniques. *Biomaterials, 26*(1), 37-46. doi: 10.1016/j.biomaterials.2004.01.063

[20] Kim, K., Luu, Y. K., Chang, C., Fang, D., Hsiao, B. S., Chu, B., & Hadjiargyrou, M. (2004). Incorporation and controlled release of a hydrophilic antibiotic using poly(lactide-co-glycolide)-based electrospun nanofibrous scaffolds. *J Control Release, 98*(1), 47-56. doi: 10.1016/j.jconrel.2004.04.009

[21] Kumbar, S. G., James, R., Nukavarapu, S. P., & Laurencin, C. T. (2008). Electrospun nanofiber scaffolds: engineering soft tissues. *Biomed Mater, 3*(3), 034002. doi: 10.1088/1748-6041/3/3/034002

[22] Li-Ya Huang, D.-G. Y., Christopher Branford-White, Li-Min Zhu. (2012). Sustained release of ethyl cellulose

micro-particulate drug delivery systems prepared using electrospraying. *Journal of material science, 47*, 1372-1377.

[23] Loo, S. C., Tan, Z. Y., Chow, Y. J., & Lin, S. L. (2010). Drug release from irradiated PLGA and PLLA multi-layered films. *J Pharm Sci, 99*(7), 3060-3071. doi: 10.1002/jps.22079

[24] Maretschek, S., Greiner, A., & Kissel, T. (2008). Electrospun biodegradable nanofiber nonwovens for controlled release of proteins. *J Control Release, 127*(2), 180-187. doi: 10.1016/j.jconrel.2008.01.011

[25] Murakami, H., Kobayashi, M., Takeuchi, H., & Kawashima, Y. (2000). Utilization of poly(DL-lactide-co-glycolide) nanoparticles for preparation of mini-depot tablets by direct compression. *J Control Release, 67*(1), 29-36.

[26] Murtaza, G. (2012). Ethylcellulose microparticles: a review. *Acta Pol Pharm, 69*(1), 11-22.

[27] N.Y. Abou-Zeid, A. I. W., N.G. Kandile, A. A. Rushdy, M. A. El-Sheikh, H. M. Ibrahim. (2011). Preparation, characterization and antibacterial properties of cyanoethylchitosan/cellulose acetate polymer blended films. *Carbohydrate Polymers, 84*(1), 223-230.

[28] Okuda, T., Tominaga, K., & Kidoaki, S. (2010). Time-programmed dual release formulation by multilayered drug-loaded nanofiber meshes. *J Control Release, 143*(2), 258-264. doi: 10.1016/j.jconrel.2009.12.029

[29] Ramasamy, T., Tran, T. H., Choi, J. Y., Cho, H. J., Kim, J. H., Yong, C. S., . . . Kim, J. O. (2014). Layer-by-layer coated lipid-polymer hybrid nanoparticles designed for use in anticancer drug delivery. *Carbohydr Polym, 102*, 653-661. doi: 10.1016/j.carbpol.2013.11.009

[30] S. Wongsasulak, M. P., J. Weiss, P. Supaphol, T. Yoovidhya. (2010). Electrospinning of food-grade nanofibers from cellulose acetate and egg albumen blends. *Journal of Food Engineering, 98*(3), 370-376.

[31] Shibata, T. (2004). Cellulose acetate in separation technology. *Macromolecular Symposia, 208*(1), 353-370.

[32] Singh, M., Shirley, B., Bajwa, K., Samara, E., Hora, M., & O'Hagan, D. (2001). Controlled release of recombinant insulin-like growth factor from a novel formulation of polylactide-co-glycolide microparticles. *J Control Release, 70*(1-2), 21-28.

[33] Streubel, A., Siepmann, J., Peppas, N. A., & Bodmeier, R. (2000). Bimodal drug release achieved with multi-layer matrix tablets: transport mechanisms and device design. *J Control Release, 69*(3), 455-468.

[34] Syeda Um-i-Zahra, X. X. S., Heyu Li, Limin Zhu. (2014). Study of sustained release drug-loaded nanofibers of cellulose acetate and ethyl cellulose polymer blends prepared by electrospinning and their in-vitro drug release profiles. *Journal of Polymer Research, 21*(12), 602.

[35] Thakur, R. A., Florek, C. A., Kohn, J., & Michniak, B. B. (2008). Electrospun nanofibrous polymeric scaffold with targeted drug release profiles for potential application as wound dressing. *Int J Pharm, 364*(1), 87-93. doi: 10.1016/j.ijpharm.2008.07.033

[36] Thitiwongsawet P, O. P., Khaoroppan A. (2010). 2,6-Dichloro-4-nitroaniline –loaded Electrospun Cellulose Acetate Fiber Mats and Their Release Characteristics.

American Journal of Chemical Engineering, 10(2), 41-47.

[37] W. Chengyao, Q. J., X. Jiangang, B.W. Christopher, Z. Limin, Y. Yang, W. Yajuan. (2011). Preparation and controlled release of degradable polymeric ketoprofen–saccharide conjugates. *Polymer Bulletin, 67*, 593-608.

[38] Wang, Y., Wang, B., Qiao, W., & Yin, T. (2010). A novel controlled release drug delivery system for multiple drugs based on electrospun nanofibers containing nanoparticles. *J Pharm Sci, 99*(12), 4805-4811. doi: 10.1002/jps.22189

[39] Weitao Zhou, J. H., Shizhong Cui, Weidong Gao. (2011). Studies of Electrospun Cellulose Acetate Nanofibrous Membranes. *The Open Materials Science Journal, 5*, 51-55.

[40] Wohl, B. M., & Engbersen, J. F. (2012). Responsive layer-by-layer materials for drug delivery. *J Control Release, 158*(1), 2-14. doi: 10.1016/j.jconrel.2011.08.035

[41] Wu, X. M., Branford-White, C. J., Zhu, L. M., Chatterton, N. P., & Yu, D. G. (2010). Ester prodrug-loaded electrospun cellulose acetate fiber mats as transdermal drug delivery systems. *J Mater Sci Mater Med, 21*(8), 2403-2411. doi: 10.1007/s10856-010-4100-y

[42] Yan, S., Xiaoqiang, L., Shuiping, L., Xiumei, M., & Ramakrishna, S. (2009). Controlled release of dual drugs from emulsion electrospun nanofibrous mats. *Colloids Surf B Biointerfaces, 73*(2), 376-381. doi: 10.1016/j.colsurfb.2009.06.009

[43] Yu, D. G., Branford-White, C., White, K., Li, X. L., & Zhu, L. M. (2010). Dissolution improvement of electrospun nanofiber-based solid dispersions for acetaminophen. *AAPS PharmSciTech, 11*(2), 809-817. doi: 10.1208/s12249-010-9438-4

[44] Yu, D. G., Shen, X. X., Branford-White, C., White, K., Zhu, L. M., & Bligh, S. W. (2009). Oral fast-dissolving drug delivery membranes prepared from electrospun polyvinylpyrrolidone ultrafine fibers. *Nanotechnology, 20*(5), 055104. doi: 10.1088/0957-4484/20/5/055104

[45] Yu, D. G., Yu, J. H., Chen, L., Williams, G. R., & Wang, X. (2012). Modified coaxial electrospinning for the preparation of high-quality ketoprofen-loaded cellulose acetate nanofibers. *Carbohydr Polym, 90*(2), 1016-1023. doi: 10.1016/j.carbpol.2012.06.036

[46] Z. Khatri, K. W., B. S. Kim, I. S. Kim. (2012). Effect of deacetylation on wicking behavior of co-electrospun cellulose acetate/polyvinyl alcohol nanofibers blend. *Carbohydrate Polymers, 87*(3), 2183–2188.

[47] Z. Ma, M. K., S. Ramakrishna. (2005). Electrospun cellulose nanofiber as affinity membrane. *Journal of Membrane Science, 265*(1-2), 115-123.

[48] Zhang, H., Wang, G., & Yang, H. (2011). Drug delivery systems for differential release in combination therapy. *Expert Opin Drug Deliv, 8*(2), 171-190. doi: 10.1517/17425247.2011.547470

[49] Zhou W, H. J., Du S, Cui S, Gao W. (2011). Electrospun Silk Fibroin/Cellulose Acetate Blend

[50] Nanofibres: Structure and Properties. *Iranian Polymer Journal, 20*(5), 389-397.